Acta Crystallographica Section C
Crystal Structure Communications
ISSN 0108-2701

Amide hydrogen bonding: control of the molecular and extended structures of two symmetrical pyridine-2-carboxamide derivatives

Orde Q. Munro* and Colin Wilson

School of Chemistry, University of KwaZulu–Natal, Private Bag X01, Scottsville 3209, South Africa
Correspondence e-mail: munroo@ukzn.ac.za

Received 24 September 2010
Accepted 6 October 2010
Online 9 October 2010

The crystal structures of two symmetrical pyridine-2-carboxamides, namely *N*,*N*′-(propane-1,3-diyl)bis(pyridine-2-carboxamide), $C_{15}H_{16}N_4O_2$, (I), and *N*,*N*′-(butane-1,4-diyl)bis(pyridine-2-carboxamide), $C_{16}H_{18}N_4O_2$, (II), exhibit extended hydrogen-bonded sequences involving their amide groups. In (I), conventional bifurcated amide–carbonyl (N—H)···O hydrogen bonding favours the formation of one-dimensional chains, the axes of which run parallel to [001]. Unconventional bifurcated pyridine–carbonyl C—H···O hydrogen bonding links adjacent one-dimensional chains to form a 'porous' three-dimensional lattice with interconnected, yet unfilled, voids of 60.6 (2) Å^3 which combine into channels that run parallel to, and include, [001]. 4% of the unit-cell volume of (I) is vacant. Compound (II) adopts a Z-shaped conformation with inversion symmetry, and exhibits an extended structure comprising one-dimensional hydrogen-bonded chains along [100] in which individual molecules are linked by complementary pairs of amide N—H···O hydrogen bonds. These hydrogen-bonded chains interlock *via* π–π interactions between pyridine rings of neighbouring molecules to form sheets parallel with (010); each sheet is one Z-shaped molecule thick and separated from the next sheet by the *b*-axis dimension [7.2734 (4) Å].

Comment

Bis(pyridine–amide) and bis(quinoline–amide) derivatives comprise a large group of organic compounds that are ideal for the mono- or dinuclear chelation of metal ions (Tsuboyama *et al.*, 1984; Chan *et al.*, 1998; Cornman *et al.*, 1999), as well as the formation of coordination polymers (Kajikawa *et al.*, 1998; van der Horst *et al.*, 2008). The basic structural features of these compounds allow them to function as multidentate *N*,*N*′-donor ligands, or as mixed *N*,*O*-donor ligands in situations where the carbonyl O atoms are used for binding. When coordinated as *N*,*N*′-donor ligands, these deprotonated diamide derivatives are typically capable of stabilizing metal ions in both high and mid-to-low oxidation states (Havranek *et al.*, 1999; Lee *et al.*, 2002). The deprotonated amide N atoms ostensibly function as hard σ-donors and such ligands exhibit a thermodynamic preference for the coordination of hard metal ions, in accord with the general principles of the HSAB (hard–soft–acid–base) theory (Pearson, 1963).

Metal-free pyridine–amides are inherently interesting from the standpoint of chemical biology. Thus, mono(pyridine-amide) analogues have well documented biological activities (Kumar *et al.*, 2007; Bonnefous *et al.*, 2005; Kakuta *et al.*, 2008). On the other hand, structural and biological studies of the analogous metal-free bis(pyridine–amides) are lacking. Notwithstanding this, and consistent with the primary function of bis(pyridine–amides) as tetradentate ligands for metal ions, Che reported significant anticancer and anti-HIV activity for several gold(III) chelates of the basic bis(pyridine–amide) ligand system in a recent patent (Che, 2004). Furthermore, ruthenium(III) nitrosyl derivatives of bis(pyridine–amides) have been studied as photoactive anticancer compounds (Patra *et al.*, 2004; Rose *et al.*, 2007, 2008). Growing interest in biological studies of the metal chelates of this class of compounds is also exemplified by reports of the interactions of vanadium(III) and oxovanadium(IV) complexes of the bis-(pyridine–amide) system with proteins (Vlahos *et al.*, 2000). As part of ongoing work in our laboratory, we have isolated crystals of two previously prepared (Barnes *et al.*, 1978), but hitherto crystallographically uncharacterized, bis(pyridine–amide) ligands, namely *N*,*N*′-(propane-1,3-diyl)bis(pyridine-2-carboxamide), (I), and *N*,*N*′-(butane-1,4-diyl)bis(pyridine-2-carboxamide), (II). For the single-crystal X-ray structures of (I) and (II) reported here, the asymmetric units comprise single and half-molecules, respectively.

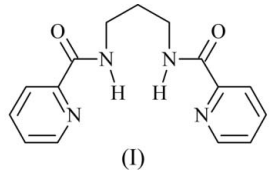

(I)

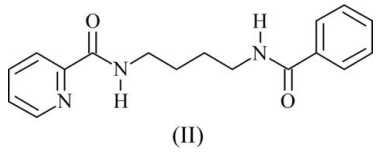

(II)

The molecular structure of (I) lacks symmetry and is located at a general position in the unit cell. The two pyridine–amide moieties, although not confined to the same plane in the crystal lattice, individually exhibit the expected near-planar geometry for a resonance-delocalized amide system (Fig. 1). The amide N—C bonds average 1.332 (9) Å, while the mean carbonyl C=O bond length is 1.232 (8) Å. These distances are slightly shorter and longer, respectively, than the typical distances found in non-amide systems (Orpen *et al.*, 1989). All other distances are normal. The amide groups are rotated slightly out of the plane of the pyridine rings, as evidenced by

 doi:10.1107/S0108270110039983

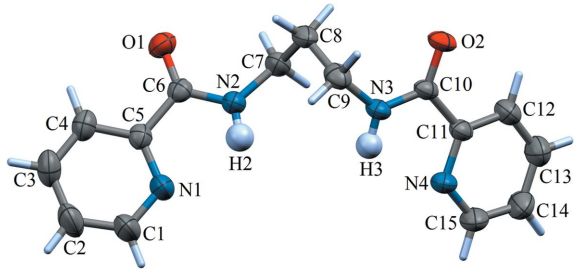

Figure 1
A view of (I), showing the atom-numbering scheme. Displacement ellipsoids are drawn at the 40% probability level for all non-H atoms, as well as for amide atoms H2 and H3; all other H atoms are rendered as end-capped cylinders.

the torsion angles N1—C5—C6—O1 and N4—C11—C10—O2, which deviate slightly from 180°, having values of 171.93 (16) and 169.13 (19)°, respectively. The dihedral angle between the two pyridine ring planes is 34.09 (16)°, with the ring centroids separated by 9.383 (2) Å.

The conformation of the propyl bridge linking the two pyridine–amide groups in (I) is not the normal staggered arrangement for an aliphatic chain. From Fig. 1, it is clear that the bridging group adopts a more twisted conformation, which allows the two amide N—H groups to point in roughly the same direction [the N—H vectors are oriented at an angle of 19 (2)° to one another]. This conformation directly reflects the extended structure of the compound (Table 1), since the two N—H groups serve as hydrogen-bond donors to one of the carbonyl O atoms, specifically O1^{i} [symmetry code: (i) x, $-y+1$, $z+\frac{1}{2}$], of a neighbouring molecule. As shown in Fig. 2, this bifurcated hydrogen-bonding pattern repeats to create a one-dimensional hydrogen-bonded chain parallel to [001]. The extended structure of (I) is made more intricate by a second, unconventional, bifurcated hydrogen bond involving carbonyl atom O2 (Table 1). In this three-centred interaction, the two hydrogen-bond donors are pyridine C—H groups of two neighbouring molecules. The combined effect of these hydrogen bonds and the conventional hydrogen bonds involving the N—H groups is the assembly of a rather open three-dimensional network structure with a pattern akin to a diamond mesh when viewed down [001]. As shown in Fig. 3, open channels run parallel to [001] at the four unit-cell corners and down the unit-cell centre. These continuous channels contain solvent-accessible voids of 60.6 (2) Å^3 (when mapped with a probe of radius 1.2 Å and a grid spacing of 0.2 Å). In principle, small molecules the size of hydrogen-bonded water (40 Å^3) could fit into voids with such dimensions. The crystals of (I) were, however, isolated as an unsolvated structure, with *ca* 4% of the unit-cell volume unoccupied. The three-dimensional network structure of (I) is presumably facilitated by (i) the flexible propyl bridge and (ii) the combination of hydrogen-bond donors/acceptors that are available. Bridge flexibility appears to be critical, since rigid aromatic bridges in bis(pyridine–amide) derivatives do not typically enable the formation of similar network structures (Fun *et al.*, 1999; Jain *et al.*, 2004). There is no evidence for π-stacking of the pyridine rings in the structure of (I), despite the expectation that such interactions might occur, given their abundance in heteroaromatic systems (Janiak, 2000).

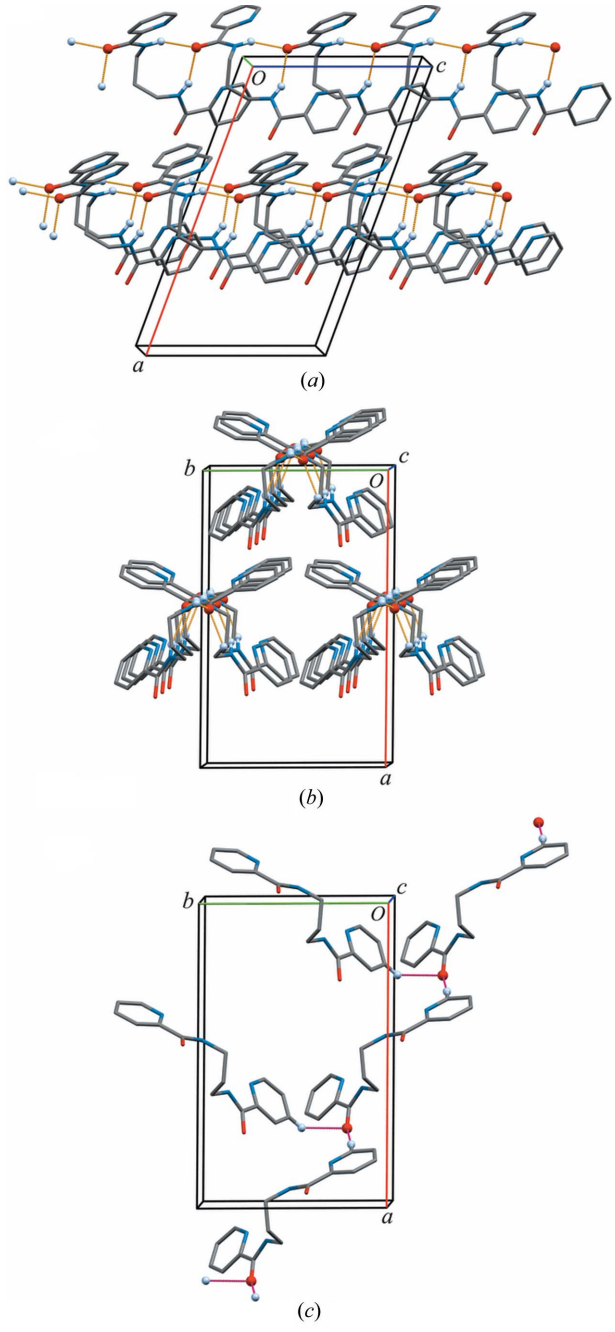

Figure 2
(*a*) Extended representation of the unit-cell contents of (I), viewed approximately down [010]. Three one-dimensional chains parallel to [001] are illustrated, with bifurcated hydrogen bonds (dashed lines; orange in the electronic version of the paper) linking neighbouring molecules. (*b*) A view of the packing diagram in (*a*), approximately down [001], highlighting the columnar nature of the hydrogen-bonded chains. (*c*) An illustration of the unconventional bifurcated hydrogen bonds (dashed lines; pink) between pyridine C—H donors and the carbonyl O atoms that are not involved in the hydrogen bonds within the one-dimensional chains shown in (*a*). These hydrogen bonds crosslink the columns shown in (*b*). Only selected interactions are shown for clarity. Atoms involved in hydrogen bonds are shown as balls of arbitrary radii. All other atoms and covalent bonds are represented as cylinders.

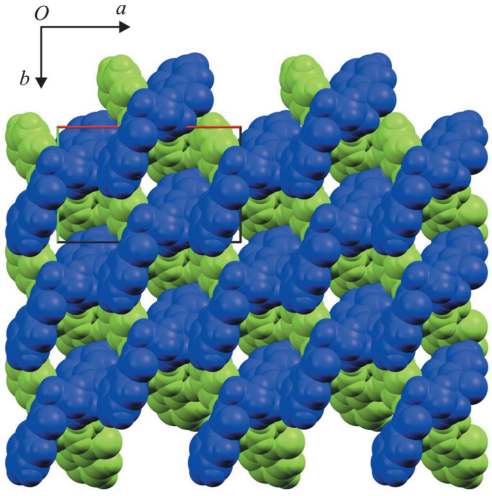

Figure 3
A space-filling view (van der Waals radii) down [001] of the crystal packing in (I). Open channels collinear with [001] are clearly visible in the lattice. Molecules have been shaded by symmetry operation.

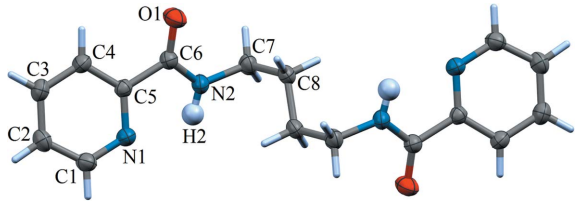

Figure 4
A view of (II), showing the atom-numbering scheme. Displacement ellipsoids are drawn at the 40% probability level for all non-H atoms, as well as for symmetry-unique amide atom H2; all other H atoms are rendered as end-capped cylinders. Atoms in the symmetry-unique half of the molecule have been labelled; the other half of the molecule is generated by the symmetry operator $(1 - x, 1 - y, -z)$.

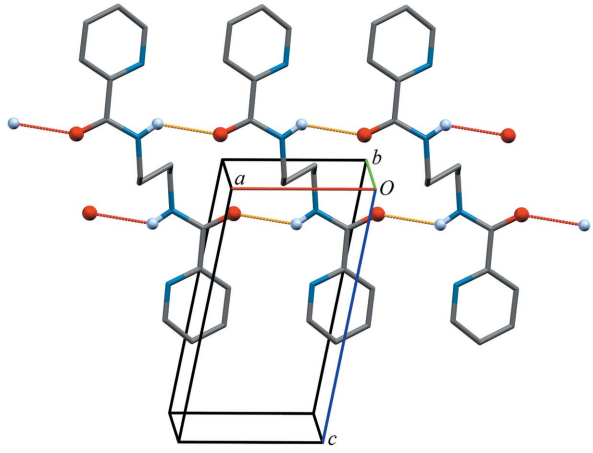

Figure 5
A representation of part of the unit-cell contents of (II), viewed approximately down [010]. Atoms involved in significant hydrogen-bonding interactions are shown as balls of arbitrary radii. All other atoms and bonds are represented as solid cylinders. Hydrogen bonds are rendered as dashed lines.

The molecule of compound (II) lies about an inversion centre (Fig. 4) which is at the mid-point of the C8—C8^{i} bond [symmetry code: (i) $1 - x, 1 - y, -z$] of the butyl bridge (*i.e.* the C_4H_8 chain). The symmetry-unique amide N—C and C═O distances are 1.3382 (12) and 1.2289 (11) Å, respectively, consistent with those of (I). Interestingly, the symmetry-unique pyridine ring and amide group are not coplanar, as evidenced by the non-zero N1—C5—C6—N2 torsion angle [−21.38 (12)°]. The out-of-plane tilt of the pyridine ring (relative to the amide group) is roughly double the average observed for the two pyridine rings in (I) and reflects a combination of two factors: (i) the formation of hydrogen bonds (N—H···O) between the amide groups of neighbouring molecules (Table 2), which leads to infinite one-dimensional chains (see below), and (ii) alleviation of unfavourable steric interactions between the closely juxtaposed pyridine rings of each monomer unit within the one-dimensional hydrogen-bonded chain, presumably as a consequence of hydrogen-bond formation. The latter notion was straightforwardly confirmed by calculating the structure of the C_i-symmetry monomer of (II) in the gas phase using density functional theory (DFT) at the B3LYP/6-31G** level of theory (Frisch *et al.*, 2004; Becke, 1993; Ditchfield *et al.*, 1971). The DFT-calculated structure of (II) has a similar butyl-chain conformation to the X-ray structure. However, the pyridine ring and amide functional groups are exactly coplanar, due to the absence of intermolecular interactions in the gas-phase structure.

The one-dimensional hydrogen-bonded chains in (II) run parallel to (010) with the chain axis collinear with [100], as shown in Fig. 5. The C8—C8^{i} bond mid-points of the assembled molecules, where atom C8^{i} is related to atom C8 by inversion, are all located in the (020) plane, such that this plane defines the spatial arrangement (one pyridine–amide unit above the plane and one below it) and directionality of the hydrogen-bonded polymer chains. Each one-dimensional chain has a distinct Z shape and interlocks with a neighbouring chain *via* intermolecular π–π interactions involving the pyridine rings (Fig. 6). Because of the layered packing of the molecules, each pyridine ring is sandwiched between two π-stacked partners. Both interactions have the usual offset antiparallel geometry with inversion symmetry (Janiak, 2000). The metrics of the interactions, where *Cg* is the centre of gravity of the pyridine ring, β the angle between the $Cg \rightarrow Cg^{i,ii}$ vector and the pyridine plane normal, IPS the interplanar separation (or perpendicular distance between *Cg* and the mean plane passing through $Cg^{i,ii}$) and LS the lateral shift (or distance between *Cg* and the perpendicular projection of *Cg* on the partner ring), are: (i) $Cg\cdots Cg^{i}$ = 3.7099 (6) Å, β = 23.0 (2)°, IPS = 3.4163 (4) Å and LS = 1.447 (2) Å [symmetry code: (i) $-x, 1 - y, 1 - z$] for the first partner ring, and (ii) $Cg\cdots Cg^{ii}$ = 3.7452 (6) Å, β = 23.6 (2)°, IPS = 3.4313 (4) Å and LS = 1.501 (2) Å [symmetry code: (ii) $-x, 2 - y, 1 - z$] for the second ring. In both cases, the interplanar separation is slightly greater than the graphite spacing of 3.35 Å (Bacon, 1951), but is nevertheless fully consistent with well defined π-stacking interactions (Hunter & Sanders, 1990).

Finally, altering the length of the carbon bridge between the amide groups in the present compounds not only permits

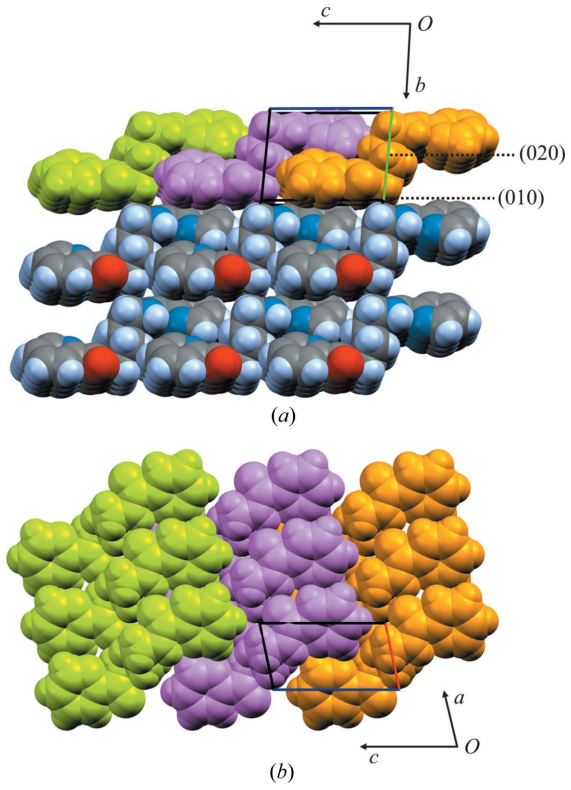

Figure 6
Space-filling views (van der Waals radii) of the one-dimensional chains that characterize the extended structure of (II). The Z-shaped π-stacked assemblies give rise to two-dimensional sheets parallel to (010) with a thickness equal to the unit-cell *b* axis. The sheet mid-point is defined by the (020) plane. The diagram in (*a*) shows three such sheets stacked along [010] in a projection approximately down [100], and the diagram in (*b*) represents the view down [010]. Individual one-dimensional hydrogen-bonded chains are highlighted with a single shade to emphasize the propagation of each chain axis along [100].

changes in the molecular conformation, but also facilitates different crystal packing architectures for each derivative. In both (I) and (II), traditional amide N—H···O hydrogen bonding is clearly the dominant interaction responsible for the extended solid-state structures. This is accompanied by unconventional C—H···O hydrogen bonding in (I) and significant pyridine–pyridine π–π stacking interactions in (II). Interestingly, the previously reported (Stephens & Vagg, 1988) ethyl-bridged bis(pyridine–amide) analogue of (I) and (II) exhibits crystallographically required inversion symmetry (space group *Pccn*) and a Z-shaped conformation akin to that of (II). Furthermore, similar sheets of N—H···O hydrogen-bonded units dominate the extended structure of the ethyl-bridged congener. The key difference, however, is that intermolecular pyridine–amide π–π interactions are favoured in the ethyl derivative because of the shorter bridge length, and each molecule thus forms hydrogen bonds with four neighbours rather than two. This establishes repeating two-dimensional N—H···O hydrogen-bond networks, or hydrogen-bonded sheets, parallel to (and including) the (010) plane. Since the individual molecules within a hydrogen-bonded sheet are oriented at 74.8° relative to those in an adjacent sheet, a herringbone packing pattern is both distinctly evident and unique to the ethyl derivative.

Deprotonated (I) and (II) are currently being used as anionic ligands for a number of metal ions in our laboratory and their coordination chemistry will be reported elsewhere.

Experimental

Compounds (I) and (II) were synthesized according to the literature method of Barnes *et al.* (1978). X-ray quality crystals of (I) were obtained by slow evaporation from a saturated solution of (I) in a chloroform–diethyl ether mixture (1:6 *v*/*v*). X-ray quality crystals of (II) formed upon slow evaporation from a saturated solution of (II) in a dichloromethane–hexane mixture (1:6 *v*/*v*).

Compound (I)

Crystal data

$C_{15}H_{16}N_4O_2$
M_r = 284.32
Monoclinic, *Cc*
a = 16.7558 (15) Å
b = 9.9188 (7) Å
c = 9.7665 (6) Å
β = 110.140 (8)°
V = 1523.9 (2) Å^3
Z = 4
Mo *K*α radiation
μ = 0.09 mm^{-1}
T = 296 K
0.65 × 0.40 × 0.15 mm

Data collection

Oxford Xcalibur 2 CCD area-detector diffractometer
Absorption correction: multi-scan [*CrysAlis RED* (Oxford Diffraction, 2008); empirical (using intensity measurements) absorption correction using spherical harmonics, implemented in the SCALE3 ABSPACK scaling algorithm]
T_{min} = 0.947, T_{max} = 0.987
7542 measured reflections
2452 independent reflections
1882 reflections with $I > 2\sigma(I)$
R_{int} = 0.023

Refinement

$R[F^2 > 2\sigma(F^2)]$ = 0.037
$wR(F^2)$ = 0.101
S = 0.98
2452 reflections
198 parameters
2 restraints
H atoms treated by a mixture of independent and constrained refinement
$\Delta\rho_{max}$ = 0.11 e Å^{-3}
$\Delta\rho_{min}$ = −0.17 e Å^{-3}

Compound (II)

Crystal data

$C_{16}H_{18}N_4O_2$
M_r = 298.34
Triclinic, $P\overline{1}$
a = 5.3215 (2) Å
b = 7.2734 (4) Å
c = 9.7993 (5) Å
α = 83.509 (4)°
β = 77.256 (4)°
γ = 81.005 (4)°
V = 364.18 (3) Å^3
Z = 1
Mo *K*α radiation
μ = 0.09 mm^{-1}
T = 296 K
0.4 × 0.4 × 0.4 mm

Data collection

Oxford Diffraction Xcalibur 2 CCD diffractometer
Absorption correction: multi-scan [*CrysAlis RED* (Oxford Diffraction, 2008); empirical (using intensity measurements) absorption correction using spherical harmonics, implemented in the SCALE3 ABSPACK scaling algorithm]
T_{min} = 0.584, T_{max} = 1.000
3732 measured reflections
2246 independent reflections
1810 reflections with $I > 2\sigma(I)$
R_{int} = 0.015

Table 1
Hydrogen-bond geometry (Å, °) for (I).

D—H···A	D—H	H···A	D···A	D—H···A
N2—H2···O1^{i}	0.92 (3)	2.08 (3)	2.8688 (18)	144 (2)
N3—H3···O1^{i}	0.85 (3)	2.18 (3)	2.931 (2)	147 (2)
C1—H1···O2^{ii}	0.93	2.47	3.397 (3)	175
C13—H13···O2^{iii}	0.93	2.58	3.366 (3)	143

Symmetry codes: (i) $x, -y+1, z+\frac{1}{2}$; (ii) $x-\frac{1}{2}, y+\frac{1}{2}, z$; (iii) $x, -y, z+\frac{1}{2}$.

Table 2
Hydrogen-bond geometry (Å, °) for (II).

D—H···A	D—H	H···A	D···A	D—H···A
N2—H2···O1^{i}	0.874 (12)	2.412 (11)	3.0901 (12)	134.8 (11)

Symmetry code: (i) $x+1, y, z$.

Refinement

$R[F^2 > 2\sigma(F^2)] = 0.044$
$wR(F^2) = 0.136$
$S = 1.11$
2246 reflections
104 parameters
H atoms treated by a mixture of independent and constrained refinement
$\Delta\rho_{max} = 0.21$ e Å^{-3}
$\Delta\rho_{min} = -0.28$ e Å^{-3}

H atoms attached to amide N atoms were located by difference Fourier synthesis and refined isotropically. The remaining H atoms were positioned geometrically and refined using a riding model, with C—H = 0.97 Å and U_{iso}(H) = 1.2U_{eq}(C) for methylene H atoms, and C—H = 0.93 Å and U_{iso}(H) = 1.2U_{eq}(C) for aromatic H atoms.

For both compounds, data collection: *CrysAlis CCD* (Oxford Diffraction, 2008); cell refinement: *CrysAlis RED* (Oxford Diffraction, 2008); data reduction: *CrysAlis RED*; program(s) used to solve structure: *SHELXS97* (Sheldrick, 2008); program(s) used to refine structure: *SHELXL97* (Sheldrick, 2008); molecular graphics: *Mercury* (CSD 2.0 Version; Macrae *et al.*, 2008); software used to prepare material for publication: *WinGX* (Farrugia, 1999).

The authors thank the University of KwaZulu–Natal and AuTEK Biomed (Mintek and Harmony) for financial support.

Supplementary data for this paper are available from the IUCr electronic archives (Reference: FG3197). Services for accessing these data are described at the back of the journal.

References

Bacon, G. E. (1951). *Acta Cryst.* **4**, 558–561.
Barnes, D. J., Chapman, R. L., Vagg, R. S. & Watton, E. C. (1978). *J. Chem. Eng. Data*, **23**, 349–350.
Becke, A. D. (1993). *J. Chem. Phys.* **98**, 5648–5652.
Bonnefous, C., Vernier, J., Hutchinson, J. H., Chung, J., Reyes-Manalo, G. & Kamenecka, T. (2005). *Bioorg. Med. Chem. Lett.* **15**, 1197–1200.
Chan, P.-M., Yu, W.-Y., Che, C.-M. & Cheung, K.-K. (1998). *J. Chem. Soc. Dalton Trans.* pp. 3183–3190.
Che, C. M. (2004). Int. Patent WO/2004/024146.
Cornman, C. R., Zovinka, E. P., Boyajian, Y. D., Olmstead, M. M. & Noll, B. C. (1999). *Inorg. Chim. Acta*, **285**, 134–137.
Ditchfield, R., Hehre, W. J. & Pople, J. A. (1971). *J. Chem. Phys.* **54**, 724–728.
Farrugia, L. J. (1999). *J. Appl. Cryst.* **32**, 837–838.
Frisch, M. J., *et al.* (2004). *GAUSSIAN03*. Revision C.02. Gaussian Inc., Wallingford, Connecticut, USA.
Fun, H.-K., Chinnakali, K., Razak, I. A., Shen, Z., Zuo, J.-L. & You, X.-Z. (1999). *Acta Cryst.* C**55**, 99–100.
Havranek, M., Singh, A. & Sames, D. (1999). *J. Am. Chem. Soc.* **121**, 8965–8966.
Horst, M. G. van der, van Albada, G. A., Ion, R.-M., Mutikainen, I., Turpeinen, U., Tanase, S. & Reedijk, J. (2008). *Eur. J. Inorg. Chem.* pp. 2170–2180.
Hunter, C. A. & Sanders, J. K. M. (1990). *J. Am. Chem. Soc.* **112**, 5525–5534.
Jain, S. L., Bhattacharyya, P., Milton, H. L., Slawin, A. M. Z., Crayston, J. A. & Woollins, J. D. (2004). *Dalton Trans.* pp. 862–871.
Janiak, C. (2000). *J. Chem. Soc. Dalton Trans.* pp. 3885–3896.
Kajikawa, Y., Azuma, N. & Tajima, K. (1998). *Inorg. Chim. Acta*, **283**, 61–71.
Kakuta, H., Zheng, X., Oda, H., Harada, S., Sugimoto, Y., Sasaki, K. & Tai, A. (2008). *J. Med. Chem.* **51**, 2400–2411.
Kumar, A., Narasimhan, B. & Kumar, D. (2007). *Bioorg. Med. Chem.* **15**, 4113–4124.
Lee, S. J., Lee, J. Y., Kim, C., Nam, W. & Kim, Y. (2002). *Acta Cryst.* E**58**, m191–m193.
Macrae, C. F., Bruno, I. J., Chisholm, J. A., Edgington, P. R., McCabe, P., Pidcock, E., Rodriguez-Monge, L., Taylor, R., van de Streek, J. & Wood, P. A. (2008). *J. Appl. Cryst.* **41**, 466–470.
Orpen, A. G., Brammer, L., Allen, F. H., Kennard, O., Watson, D. G. & Taylor, R. (1989). *J. Chem. Soc. Dalton Trans.* pp. S1–S83.
Oxford Diffraction (2008). *CrysAlis CCD* and *CrysAlis RED*. Versions 1.171.32.24. Oxford Diffraction Ltd, Yarnton, Oxfordshire, England.
Patra, A. K., Rose, M. J., Murphy, K. A., Olmstead, M. M. & Mascharak, P. K. (2004). *Inorg. Chem.* **43**, 4487–4495.
Pearson, R. G. (1963). *J. Am. Chem. Soc.* **85**, 3533–3539.
Rose, M. J., Fry, N. L., Marlow, R., Hinck, L. & Mascharak, P. K. (2008). *J. Am. Chem. Soc.* **130**, 8834–8846.
Rose, M. J., Olmstead, M. M. & Mascharak, P. K. (2007). *J. Am. Chem. Soc.* **129**, 5342–5343.
Sheldrick, G. M. (2008). *Acta Cryst.* A**64**, 112–122.
Stephens, F. S. & Vagg, R. S. (1988). *Inorg. Chim. Acta*, **142**, 43–50.
Tsuboyama, S., Sakurai, T., Kobayashi, K., Azuma, N., Kajikawa, Y. & Ishizu, K. (1984). *Acta Cryst.* B**40**, 466–473.
Vlahos, A. T., Tolis, E. I., Raptopoulou, C. P., Tsohos, A., Sigalas, M. P., Terzis, A. & Kabanos, T. A. (2000). *Inorg. Chem.* **39**, 2977–2985.